



# Development of an automated flow chemistry affinity-based purification process for DNA-encoded chemistry

Robin Dinter<sup>1</sup> · Katharina Götte<sup>2</sup> · Franziska Gronke<sup>1</sup> · Leon Justen<sup>1</sup> · Andreas Brunschweiger<sup>3</sup> · Norbert Kockmann<sup>1</sup>

Received: 8 May 2023 / Accepted: 14 August 2023 / Published online: 26 September 2023  
© The Author(s) 2023

## Abstract

An automated flow chemistry platform for DNA-encoded library (DEL) technologies requires the integration of a purification process for DNA-tagged substrates. It facilitates the development of further DEL reactions, building block rehearsal, and library synthesis. Therefore, a recently developed, manual affinity-based batch purification process for DNA-tagged substrates based on dispersive solid-phase extraction (DSPE) was transferred to automated flow chemistry using tailored 3D-printed microfluidic devices and open-source lab automation equipment. The immobilization and purification steps use Watson–Crick base pairing for a compound-encoding single-stranded DNA, which allows for the thorough removal of impurities and contaminations by washing steps and operationally simple recovery of the purified DNA-encoded compounds. This work optimized the annealing step for flow incubation and DNA purification was accomplished by flow DSPE washing/elution steps. The manually performed batch affinity-based purification process was compared with the microfluidic process by determining qualitative and quantitative DNA recovery parameters. It aimed at comparing batch and flow purification processes with regard to DNA recovery and purity to benefit from the high potential for automation, precise process control, and higher information density of the microfluidic purification process for DNA-tagged substrates. Manual operations were minimized by applying an automation strategy to demonstrate the potential for integrating the microfluidic affinity-based purification process for DNA-tagged substrates into an automated DNA-encoded flow chemistry platform.

**Keywords** DNA-encoded chemistry · DNA purification · Dispersive solid-phase extraction (DSPE) · Affinity-based purification · Microfluidic · Flow chemistry · 3D-printed lab equipment · Open-source lab automation

## Introduction

DNA-encoded library (DEL) technology is one of the leading screening technologies for identifying small biologically active molecules. Compounds are identified from DELs based on their DNA-sequence [1–3]. DELs are typically synthesized by iteration of combinatorial chemical reaction cycles, and ligation of DNA fragments for the construction of DNA-barcode [4, 5]. DELs offer an alternative to costly high-throughput screening (HTS) in drug discovery [1, 6]. DNA-tagged reaction

products are purified prior to analysis by manual pipetting and classical batch processes such as ethanol precipitation, ion-pair high performance liquid chromatography (HPLC), and ion-exchange chromatography [7–11]. The advantages and limitations of these purification processes have been discussed in the literature on DEL purity [5, 9, 12–14]. To establish a new affinity-based purification method for DNA-tagged substrates, Götte *et al* [5, 12] adopted prior knowledge of DNA-encoded chemistry on a solid-phase, called controlled pore glass (CPG) of the Brunschweiger group [1–3, 6, 15], as well

✉ Norbert Kockmann  
norbert.kockmann@tu-dortmund.de  
Andreas Brunschweiger  
andreas.brunschweiger@uni-wuerzburg.de

<sup>1</sup> Department of Chemical and Biochemical Engineering, Laboratory of Equipment Design, TU Dortmund University, Emil-Figge-Str. 68, 44227 Dortmund, Germany

<sup>2</sup> Department of Chemistry and Chemical Biology, Medicinal Chemistry, TU Dortmund University, Otto-Hahn-Str. 6, 44227 Dortmund, Germany

<sup>3</sup> Department of Chemistry and Pharmacy, Institute for Pharmacy and Food Chemistry, Julius-Maximilians-University of Würzburg, Am Hubland, 97074 Würzburg, Germany

as the affinity-based purification of mRNA by Gagnon *et al.* [7, 16, 17], based on dispersive solid-phase extraction (DSPE). In this process, DSPE is a chemical-physical principle of solid-phase extraction (SPE), in which the solid-phase is not stationary fixed but dispersed in the solution [18, 19]. The idea of this affinity-based purification process for DNA is that a single-stranded (ss)DNA was bound to a solid-phase, called matrix, to subsequently bind a complementary compound-encoding DNA-sequence via Watson–Crick interactions [5]. Then, contaminations are thoroughly removed by washing steps with a range of solvents and buffers, while the DNA remained bound on the solid-phase, as shown in Fig. 1.

Figure 1 explains the four steps of annealing, washing, elution, and drying of the DSPE process modified for DNA-substrates according to Götte *et al.* [5, 12]. A 14mer fully complementary ssDNA-2a was labeled with a fluorophore to ssDNA-2b for in-process control. DNA-2b was used as a model analyte-DNA for a DNA-tagged compound representing a DNA reaction product after DEL-synthesis. Agarose particles form the agarose-matrix as solid-phase. A copper-catalyzed alkyne-azide cycloaddition reaction (ESI Scheme S 1), coupled a complementary 14mer ssDNA to the solid agarose-matrix to form the **capture-DNA-1**. The first step of the DSPE process is the annealing step, in which the **analyte-DNA-2b** was immobilized to the adsorbent

**capture-DNA-1** by Watson–Crick interaction. This step depends on the buffer solution and incubation conditions, such as temperature and time (ESI Section "Section 2.2"). For the second step, the washing step, the bound matrix-analyte-complex was transferred to a filter column with a pore size below the particle size of the agarose-matrix. Then, the contaminations were removed from the bound matrix-analyte-complex under highly stringent washing conditions using a range of washing solvents of decreasing polarities and optionally buffers to remove metal contaminations [6, 15]. According to Götte *et al.* [5, 12], the optimized washing conditions (ESI Figure S 1) include purified water ( $dH_2O$ ) to separate all water-soluble components and to fix the matrix-analyte-complex on the filter. Next, ethylenediaminetetraacetate (EDTA) removed metal ions, and residues were rinsed out again by  $dH_2O$ . Subsequently, organic solvents with different polarities removed contaminants of different polarities and solubilities. The washing solvents included dimethylformamide (DMF), methanol (MeOH), acetonitrile (MeCN), and dichloromethane ( $CH_2Cl_2$ ). In the next step of DSPE, the purified DNA-2b was eluted from the complementary **capture-DNA-1** using 32% aqueous solution of  $NH_3$  as the elution solvent and dried by evaporation.

In previous work of our groups [5], automation of the repetitive and laborious washing/elution steps of the established

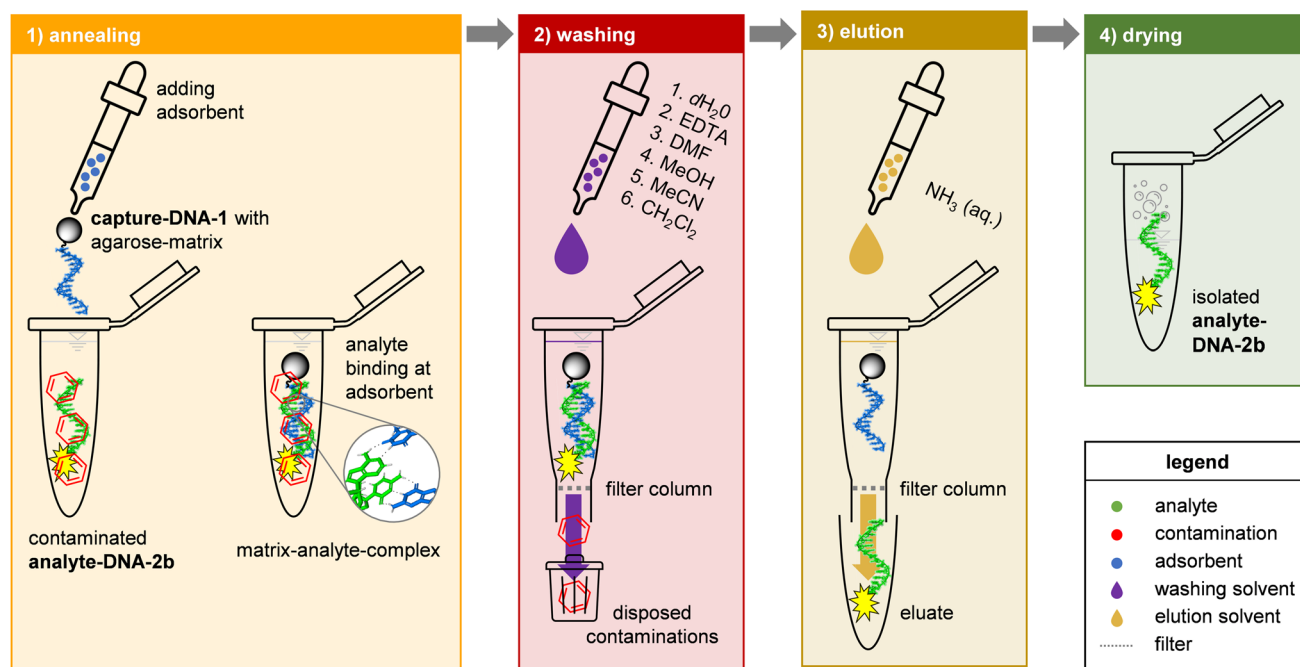


**Fig. 1** Dispersive solid-phase extraction (DSPE) process for DNA-tagged substrates established by Götte *et al.* [5]. The first step is annealing, in which the contaminated, compound encoding **analyte-DNA-2b** was bound via Watson–Crick interactions to the **capture-DNA-1** containing the agarose-matrix (solid-phase). In the second step, six different washing solvents with different

polarities remove the contaminations sequentially, while a filter retains the solid-phase. In the elution step, the elution solvent separates the purified compound-encoding DNA from the solid-phase. In the last step, the purified **analyte-DNA-2b** was isolated by evaporating solvent residuals and can be used again for further DEL synthesis steps

affinity-based purification was effectively performed in batch mode using 96-microwell filter plates and 3D-printed tailored vacuum chambers. This demonstrated that the established purification process was robust enough for batch automation and provided comparable DNA recoveries with high precision as the manually purified analyte-DNA [5]. This motivated us to proceed one step further and transfer the batch process into an automated flow process. This work is framed by the ambition to create an integrated, efficient, and automated microfluidic platform for DNA-encoded chemistry, including preparation, reaction, purification, and analysis steps. This approach combines two leading technologies and the DEL synthesis benefits from the advantages of flow chemistry, e.g., the potential for precise process control and higher efficiency [18, 20]. As a first step towards the DNA-encoded flow chemistry platform, Dinter *et al* [4], successfully transferred the amide coupling reaction with DNA-tagged substrates into a microfluidic reactor system using 3D printing and open-source automation. In addition to the reaction transfer, the purification steps of the DNA reaction mixture prior to analysis are equally necessary for an integrated and automated microfluidic DEL-synthesis platform. This work addresses the significant challenge of achieving high-quality DNA in encoded products to avoid the carry-over of reagents into subsequent synthesis steps by removing contaminations through a microfluidic affinity-based purification process for DNA. A few publications have already investigated microfluidic and flow chemistry affinity-based compound purification but without DNA-tagged substrates or DEL reaction mixtures [18, 21]. This work focused on transferring affinity-based batch purification to flow chemistry, and aimed to obtain comparable batch and flow results regarding DNA purity and DNA recovery using model analyte-DNA. First, the annealing step was optimized for flow incubation by solving the key challenges of shaking and heating analyte-DNA and handling the solid agarose-matrix particles in the microchannel. The robust application of the flow annealing concept was confirmed using longer ssDNA. Next, the flow washing/elution concepts were developed by optimizing the DNA purity and excluding cross-contaminations and DNA loss in the microchannel. Finally, both microfluidic annealing and washing/elution concepts were combined and automated by tailored microfluidic sensors and actuators with open-source hard- and software to minimize manual operations. This demonstrates the potential for integrating the microfluidic affinity-based purification process into an automated DNA-encoded flow chemistry platform.

## Results and discussion

This work adapted an optimized affinity-based batch purification procedure for DNA-labelled substrates developed by Götte *et al* [5], to an automated microfluidic concept.

The annealing, washing, and elution steps were transferred to an automated microfluidic purification concept. The remaining drying and analysis steps (Fig. 1) were still performed manually with a vacuum centrifuge and UV–Vis spectroscopy. The analytic process for DNA recovery is briefly discussed before describing the process design and evaluating the flow concepts.

### Analytical process for DNA recovery

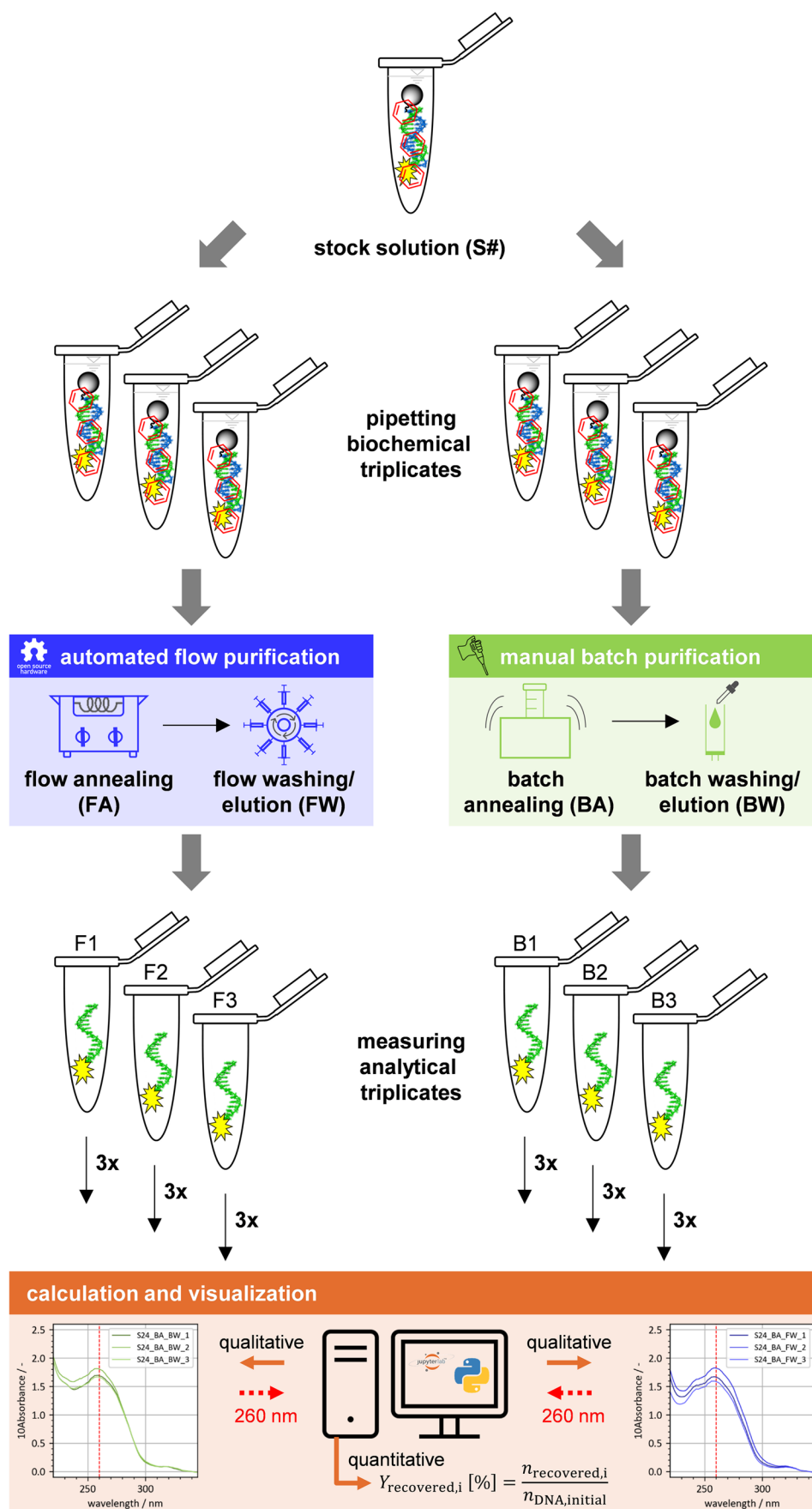
For all model analyte-DNA to be purified and analyzed, the initial DNA amount before purification was 500 pmol, which presents the target value of comparing the flow with the batch process. The stock solutions with 500 pmol initial DNA amount were prepared by performing the procedure, as explained in ESI Section 2.1. Here, the analyte-DNA to be purified and the capture-DNA were pipetted from a stock solution and represented an aliquot from a stock solution, as shown in Fig. 2. Due to variations in the composition of the agarose-matrix, the samples must be taken from the same stock solution to investigate and compare the affinity-based purification process in batch and flow, as explained in detail in the ESI Section 3.1.4. Six replicates were prepared from the same stock solution to achieve statistically relevant results. Three samples were purified in batch (B1, B2, B3) for reference, and three samples were purified in flow (F1, F2, F3), as presented in (Fig. 2).

To evaluate the automated microfluidic affinity-based purification process and the head-to-head comparison of flow and batch process, the UV–Vis spectrum of the total absorbance was measured three times for each sample (e.g., B1.1, B1.2, B1.3) to obtain analytical triplicates. The results were dimensionless absorbance spectra from 230 nm (A230) to 280 nm (A280) with the absorption maximum of DNA at 260 nm (A260), which is typical for nucleic acids [22]. The DNA purity as a qualitative indicator is expressed in terms of the absorption ratios of a sample (e.g. A260/A280), as explained in ESI. In addition further quantitative parameters were calculated using OligoCalc [23] and the characteristic DNA peak (A260) of the absorption spectra, as described in ESI. With these qualitative and quantitative parameters, the DNA recovery can be evaluated and compared between batch and the flow affinity-based purification process.

### Flow annealing concept

The initial focus of this study was to transfer the discontinuous annealing step into a flow annealing concept. Previous studies on the batch purification process have investigated different solid support materials, the stability of the

**Fig. 2** Scheme of sample distribution and measurement procedure. The stock solution (S#) contained the analyte-DNA and the capture-DNA. Six biochemical replicates were taken from the stock solution. Three samples were used in the reference affinity-based batch purification process (B1, B2, B3), and three samples were used in the newly developed affinity-based flow purification process (F1, F2, F3). After purifying all samples in batch and flow, each sample (B1) was measured three times using UV–Vis spectroscopy (e.g., B1.1, B1.2, B1.3) to obtain analytical replicates. The measured absorbance spectra were stored in a data structure and proceeded by Python calculations



matrix-analyte-complex under washing conditions, and the impact of incubation temperature and time on binding the **DNA-2b** to the complementary **capture-DNA-1** [5, 12]. This work served as a starting point for investigating an affinity-based flow purification process. The first technical challenge for the flow purification process of parallel shaking and heating of batch samples on a thermal shaker were solved by pumping the flow sample through a fluoroethylene propylene (FEP) tube tempered in a water bath. However, one of the most crucial challenges was handling the solid bead particles of the sample. This results in a suspension of agarose-matrix particles with a size of 50–150  $\mu\text{m}$  tending to sediment in the stock solution after only 5 s (ESI Section 3.1.4). Therefore, mixing the sample homogeneously and transferring it to a microfluidic process without leaving particles in the microchannel was challenging, which would have reduced the stringency of purification and recovery of DNA. This was accomplished by pumping the samples back and forth through the FEP-tube for a prespecified heating and cooling time. Preliminary studies investigated the impact of the inner channel diameter on sedimentation, as shown in ESI Section 3.1.4. The overview and experimental setup of the flow annealing concept are shown in Fig. 3 A,B. To ensure successful incubation of **capture-DNA-1**, fluorescence-labeled **DNA-2b** was used that was visible in the FEP-tube during the flow process (Fig. 3 C).

In Fig. 3 A,B, the sample containing the **analyte-DNA-2b** and the **capture-DNA-1** was mixed and pumped into the microfluidic system. The thermal shaker of the batch annealing concept was replaced by a tempering water bath and a FEP-tube with a total length of 2.8 m. After primarily studying the inner channel diameter to avoid sedimentation of the sample inside the FEP-tube (ESI Section 3.1.4), an inner channel diameter of 1.6 mm was chosen. The channel was classified into the first section of 0.2 m, where the sample was introduced into the microfluidic system, followed by a coiled section of 1.0 m for incubating the sample in the water bath. After incubation, the sample was cooled to room temperature (RT) in another coiled FEP-tube of 1.6 m outside the water bath. The detailed protocol and procedure are described in the ESI Section 3.1.3. Figure 3 C shows the sample after successfully incubating and forming the analyte-matrix-complex by Watson–Crick interactions. In addition, Fig. 3 C confirms that no sedimentation of the sample was seen during flow annealing, as the most intense discoloration occurs in the vicinity of the agarose-matrix. A negative example where sedimentation occurs in FEP-tubes with smaller channel diameters is given in the ESI Section 3.1.4. After successfully annealing of the DNA oligonucleotides in flow, the sample was loaded onto a filter column (C1) for subsequent washing/elution.

Next, the volumetric flow rate as a potentially relevant parameter, the robustness (incubation temperature, longer

analyte-ssDNA oligonucleotides) of the flow annealing concept, and the qualitative and quantitative DNA recovery parameters defined previously were characterized by the following set of experiments. These experiments aim at achieving comparable recoveries of the purified **DNA-2b** by flow and batch purification. Two triplicates ( $2 \times 3$  samples) were prepared from the same stock solution (S), as explained in Fig. 2. The first triplicate was discontinuously annealed in batch (BA), and the second triplicate was continuously annealed in flow (FA). Finally, further purification steps, such as washing/elution, were performed in batch (BW) to directly compare the batch and flow annealing regarding DNA recovery and purity. Figure 4 shows the results of transferring the discontinuous annealing step to a continuous microfluidic concept with the relevant parameters.

In the first set of experiments, the effect of the volumetric flow rates on the annealing quality was evaluated in a range of 0.8–3.6  $\text{mL min}^{-1}$  (Fig. 4 A). Looking first at the average UV–Vis spectra of each sample as a quantitative parameter in Fig. 4 A-a), all samples show the characteristic peak at the wavelength A260 and the valley at the wavelength A240. This indicated the successful development of DNA annealing in flow. The individual results of each analytical batch and flow triplicate can be found in the ESI Table S 4. To examine qualitative DNA recovery and the effect of increasing volumetric flow rates, the averaged **DNA-2b** recoveries of the triplicated samples after flow annealing (FA) were calculated and visualized in the bar chart in Fig. 4 A-b). The same pattern in the bar plot represents the corresponding batch recoveries of the same stock solution. At the lowest volumetric flow rate of 0.8  $\text{mL min}^{-1}$ , DNA recovery was lowest at  $360 \pm 75$  pmol and a significant deviation of 21% from the batch reference, as confirmed in the parity plot (Fig. 4 A-c)). If the volumetric flow rate was increased by 0.7  $\text{mL min}^{-1}$ , the recovery **DNA-2b** was increased to  $458 \pm 26$  pmol. In the parity plot, the deviation from the batch reference was still too high, which is illustrated by the fact that samples from stock solution S17 were in the upper margin of the valid precision range of 20%. However, a further increase in the volumetric flow rate did not yield higher **DNA-2b** recoveries, and the sample annealed at 2.2  $\text{mL min}^{-1}$  was in the same upper margin of the parity plot. The highest amount of recovered **DNA-2b** in this set of experiments was yielded at 2.9  $\text{mL min}^{-1}$  with  $468 \pm 38$  pmol, showing the lowest deviation from the batch reference, as confirmed in the parity plot. A further increase in flow rate to 3.6  $\text{mL min}^{-1}$  caused a decrease of the recovered **DNA-2b** to  $366 \pm 15$  pmol, as controlled incubation was no longer possible. This effect was confirmed and observed by increasing the volumetric flow rate above 3.6  $\text{mL min}^{-1}$ , but was not further investigated in this study. The first set of experiments showed that reproducible and comparable **DNA-2b** recoveries were achieved by the

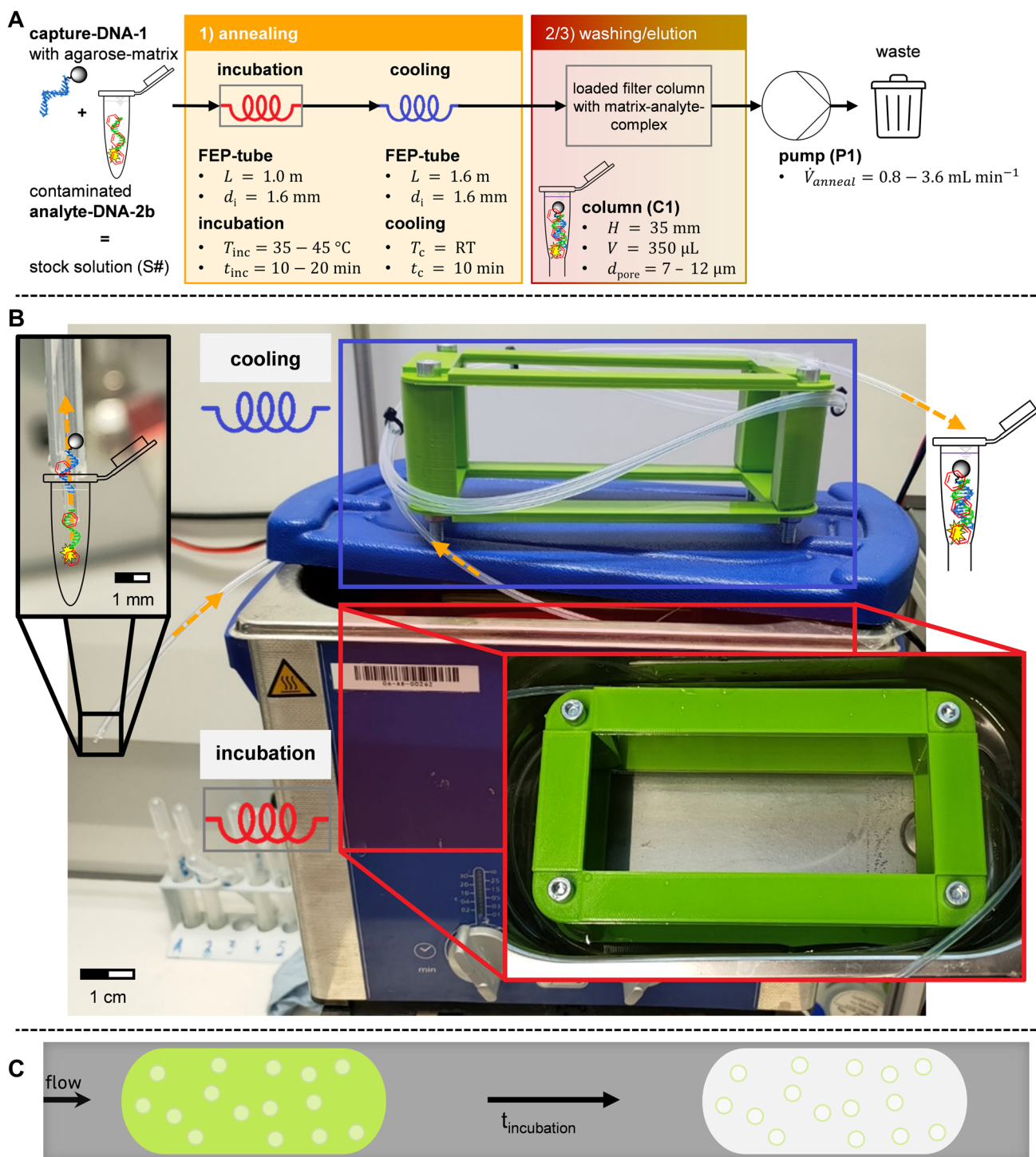


**Fig. 3** Overview and experimental setup of the flow annealing concept. **A**) Schematic structure of microfluidic DNA annealing, including two tempering coiled loops for incubation (heating) and cooling. The stock solution were pumped as a slug into the microchannel and incubated for a defined temperature and time, depending on the set of experiments. After incubation, the matrix-analyte complex was cooled at room temperature (RT) and loaded into a

filter column (C1) for washing/elution. **B**) Experimental setup, the arrows indicate the flow direction of the analyte-DNA taken from stock solution. The FEP-tube was coiled around a rack and immersed in a water bath for heating. **C**) Procedure of incubation and immobilizing the fluorescent DNA-2b (green-yellow staining) to the capture-DNA-1 as the most intense discoloration indicated successful binding

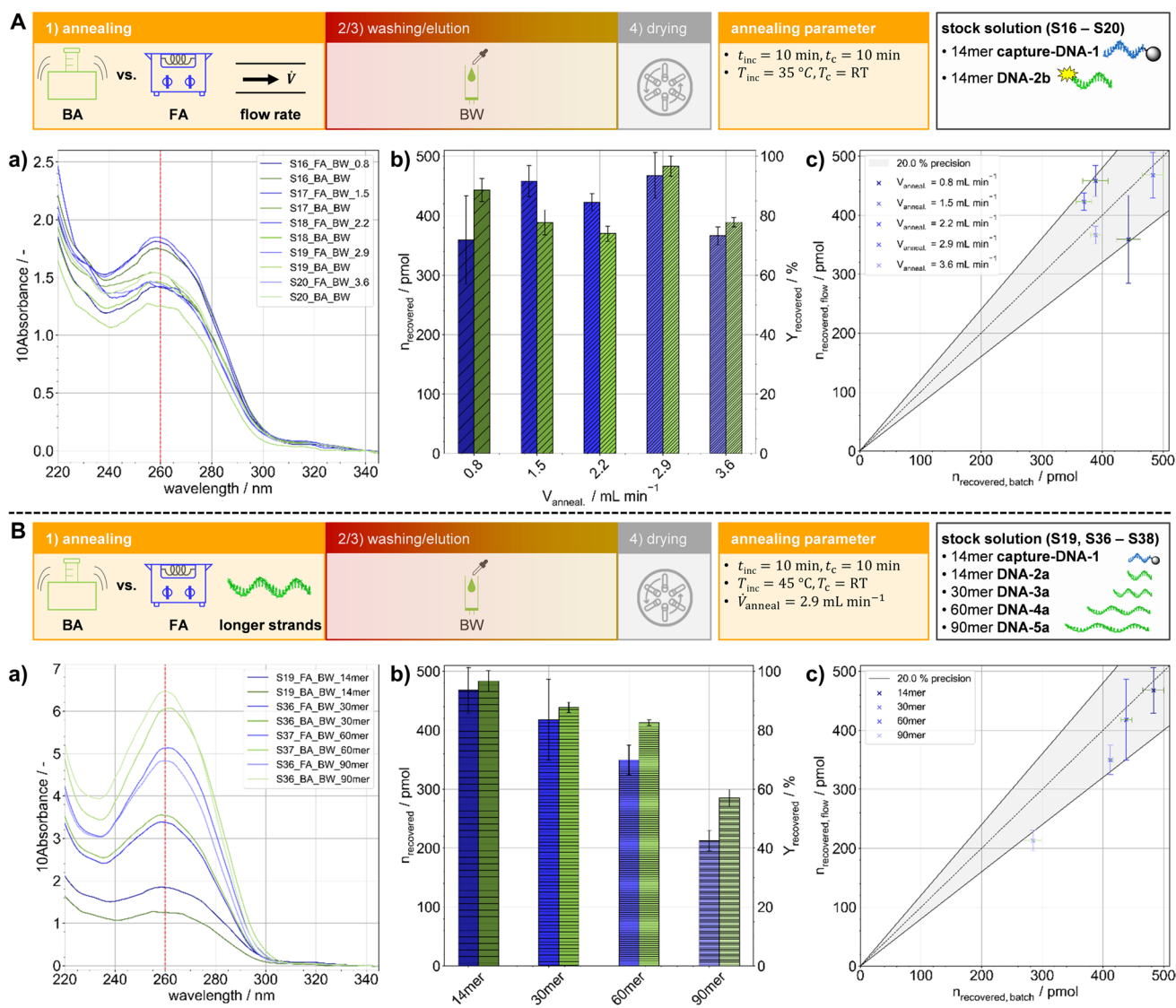


**Fig. 4** Characterization, comparison, and robustness of the relevant parameters on flow annealing concept. The triplicates from the stock solutions (S#) containing the **analyte-DNA-2b** (500 pmol) and the **capture-DNA-1**. They were continuously annealed in flow (FA) and discontinuously annealed in batch (BA). All further affinity-based purification steps, such as washing/elution, were carried out in batch (BW) to compare both annealing modes directly: **a)** UV-Vis absorbance spectrum with quantitative DNA recovery; **b)** bar-plot with qualitative DNA recovery ( $n_{recovered}$  in pmol,  $Y_{recovered}$  in %) calculated

by the absorbance spectrum at A260; **c)** parity-plot for comparing the qualitative DNA recovery after flow and batch annealing. **A)** Investigation of five increasing volumetric flow rates on the flow annealing (FA) by incubating the sample for 10 min at 35 °C in flow (blue colors). Compared with corresponding batch annealed (BA) samples using the same incubation conditions (green colors). **B)** Robustness of the flow annealing using longer analyte-ssDNA with increasing base numbers (**DNA-2a** = 14mer, **DNA-3a** = 30mer, **DNA-4a** = 60mer, **DNA-5a** = 90mer) and the same **capture-DNA-1** (14mer)

volumetric flow rate at 2.9 mL min<sup>-1</sup>, as it ensured sufficient mixing of the sample and contact time of **capture-DNA-1** with **analyte-DNA-2b**. Thus, the volumetric flow rate was set to 2.9 mL min<sup>-1</sup> for flow annealing (FA) in the following experiments.

After verifying the feasibility of the flow annealing concept for DNA-tagged substrates, the applicability for longer ssDNA-strands as analyte-DNA was investigated. This step will be important to make affinity-based purification

applicable to the different steps in a DEL synthesis, which are accompanied by the growing DNA chain. The samples were prepared analogously to the previous experiments with 14mer **analyte-DNA-2a**, only that longer DNA oligonucleotides were used containing a partial sequence complementary to the **capture-DNA-1** (Fig. 4 B). First, a 30mer **DNA-3a** was annealed in parallel continuously in flow (FA) and discontinuously in batch (BA) by incubating the sample at 45 °C for 10 min. The incubation temperature was increased

from 35 °C to 45 °C for this set of experiments to verify that the flow annealing concept was robust at varying temperatures, as previously shown by Götte *et al.* [5, 12]. The same procedures were repeated for 60mer **DNA-4a** and 90mer **DNA-5a**. The results shown in Fig. 4 B-a) indicated that these longer DNA-strands were purified in the same way as a fully complementary analyte-DNA (14mer). Examination of qualitative DNA parameters (Fig. 4 B-b) shows that the DNA recovery for longer strands of analyte-DNA decreased from  $483 \pm 17$  pmol (14mer **DNA-2a**) to  $285 \pm 14$  pmol (90mer **DNA-5a**) for the reference batch annealing. The same trend was seen for the flow annealing concept, where 14mer **DNA-2a** yielded  $468 \pm 38$  pmol after purification and recovery decreased to  $213 \pm 17$  pmol for 90mer **DNA-5a**. The decreasing trend is confirmed using manually batch affinity-based purification [12] and underlines the correct transfer of batch to flow annealing process. The parity plot (Fig. 4 B-c) verifies this decreasing trend and points out that the DNA recovery with a longer-stranded analyte-DNA was lower in flow than in batch. For 60mer **analyte-DNA-4a** and 90mer **analyte-DNA-5a**, the DNA recoveries were in the lower margin of the valid precision range. Thus, the previously designed process was suitable for up to 60mer analyte-DNA oligonucleotides. Supposing that recovery of longer DNA-strands is required for further application, longer capture-DNA oligonucleotides will be tested, such as a 20mer. In addition, the incubation and cooling temperature, as well as the related process time, might have been too low for longer-stranded analyte-DNA [12].

For the first time, it has been demonstrated that the annealing step of the affinity-based purification process for DEL technologies was transferable into a microfluidic process. Nevertheless, this set of experiments demonstrated the application and transfer to the flow annealing concept using longer DNA strands and showed comparable trends to the batch experiments for DNA purity and recovery. Furthermore, this second set of experiments clearly demonstrated the robustness and limitations of the newly designed flow annealing process using 14mer **capture-DNA-1** for DNA-tagged substrates and that longer capture-DNA oligonucleotides were required for longer analyte-DNA sequences.

### Flow washing/elution concept

Following the successful demonstration of the microfluidic annealing concept with fluorescence-labeled **DNA-2b** annealed to the fully complementary single-stranded **capture-DNA-1**, this section focuses on the transfer of the washing/elution steps of the DSPE (Fig. 1) to a flow washing concept for purifying the contaminated analyte-DNA. Here, it is essential that the washing solvents do not disrupt the Watson–Crick interaction of analyte and capture-DNA. First, the solvents must be dosed onto the filter column (C1) in a specific order

and volume. In batch mode, this was done by manual pipetting, but in flow mode, a tailored multi-port valve (V1) controlled by open-source hardware was applied. The valve (V1) consists of a NEMA 23 stepper motor and a tailored shaft coupler with an adapter for a multi-port valve (V1). The technical drawings, construction, and detailed information about the tailored multi-port valve (V1) are included in the ESI Section 3.2.2. Second, for pumping the solvents onto the filter column (C1) and ensuring that the sample was in contact with the solvents, a vacuum chamber was used in batch mode, according to the purification protocol. In flow mode, the solvents were pumped to the filter column (C1) using a peristaltic pump (P1). The overview of the experimental flow washing/elution setup is illustrated in Fig. 5.

The washing/elution solvents were stored in 10 mL syringes connected directly to the multi-port valve (V1).  $\text{CH}_2\text{Cl}_2$  was stored in a 5 mL glass syringe on ice, as its low vapor pressure could lead to gas formation and thus inaccurate dosing [24]. Between the solvents,  $d\text{H}_2\text{O}$  and ambient air were used to prevent mixing or dilution of the pure organic solvents, as discussed in the ESI Section 3.2.4. Next, the filter column (C1) containing the contaminated analyte-DNA was connected to outlet port 9 of the multi-port valve (V1). The volume of each solvent was increased from 600  $\mu\text{L}$  in batch to 650  $\mu\text{L}$  in flow to ensure that the solvents completely wet the filter column (C1) and to compensate for the dead volume between the syringe screw connection and the multi-port valve (V1). After washing,  $2 \times 250 \mu\text{L}$   $\text{NH}_3(\text{aq.})$  was dosed at a volumetric flow rate of  $0.8 \text{ mL min}^{-1}$  through the same multi-port valve (V1) at port 8 to elute the analyte-DNA. The volumetric flow rate of the elution solvent  $\text{NH}_3(\text{aq.})$  was not changed in the following set of experiments, since a low flow rate was required to account for the low vapor pressure of aqueous ammonia of 0.837 bar at 20 °C [25]. Finally, a tailored three-port valve (V2) controlled by a servo motor and automated with open-source hardware separated the used washing solvents with the contaminations from the purified analyte-DNA (ESI Section 3.2.2). After complete washing/elution, the remaining elution solvent was subsequently evaporated in the discontinuous drying step to obtain the purified and isolated analyte-DNA (Fig. 1, and ESI Section 2.5).

Before examining the qualitative and quantitative DNA recovery parameters affects the flow purification, it needed to make sure the error-free functionality of the newly developed microfluidic washing/elution for DNA-tagged substrates. In these preliminary experiments (ESI Section 3.2.4), it was validated that no cross-contamination and no loss of analyte-DNA occurred in the microfluidic system. To reduce the effect of direct contact between the pure organic solvents affecting DNA recovery, ambient air was used between solvent changes, as discussed in ESI Section 3.2.4.. After successfully verifying the error-free functionality of the microfluidic washing/elution concept, the relevant parameters (volumetric flow

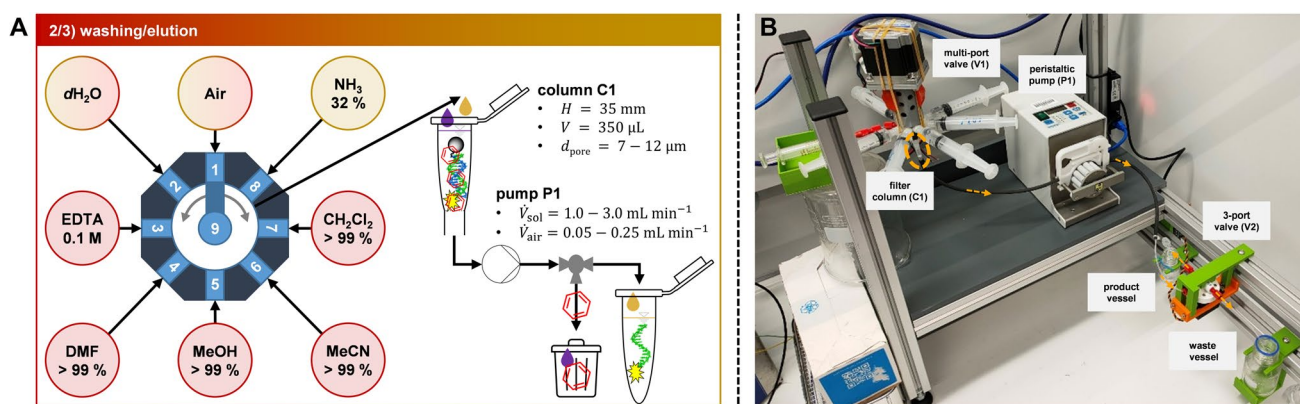


**Fig. 5** Overview and experimental setup of the flow washing/elution concept. **A** Schematically structure of microfluidic washing/elution, including washing (red frames) and elution solvents (yellow frames).  $d\text{H}_2\text{O}$  and air were used for both steps and marked with red-yellow frames. The washing/elution solvents from the storage vessels were pumped (P1) through a multi-port valve (V1) to the filter

column (C1), which was loaded with the analyte-matrix complex after annealing. Downstream of the filter column (C1), the dispersed contaminations and residuals were pumped to the waste (washing step), or the eluate was pumped to the product vessels (elution step). **B** Experimental setup, where the arrows indicate the flow direction of the washing/elution solvents

rate of the washing) affecting the purity and recovery of the analyte-DNA were characterized.

The following experiments aimed at achieving comparable recoveries of purified **DNA-2b** using the flow and batch affinity-based purification process. Two triplicates ( $2 \times 3$  samples) were prepared from the same stock solution, as shown in Fig. 2. The first triplicate was discontinuously washed in batch (BW), and the second triplicate was continuously washed in flow (FW). The preceding annealing step was performed in batch (BA) to directly compare batch and flow washing/elution regarding the affinity-based purification process stringency. Figure 6 shows the results of transferring the discontinuous washing/elution steps to a continuous microfluidic washing/elution concept with the relevant parameters.

The first set of experiments (Fig. 6 A) investigated the three increasing volumes (50, 150, 250  $\mu\text{L}$ ) of ambient air to separate the pure organic washing solvents and their impact on the flow washing DNA recovery. Preliminary tests had already shown that pumping ambient air between the seven solvents prevented solvent mixing and improved DNA recovery in the flow process achieving comparable DNA recoveries between batch and flow (ESI Section 3.2.4). Looking first at the average UV-Vis spectra of each sample as a quantitative parameter in Fig. 6 A-a), all samples show the characteristic peak at 260 nm wavelength (A260) and the valley at 240 nm wavelength (A240). This indicated that the discontinuous washing steps were successfully transferred to the flow concept (ESI Table S 4). Looking more closely at the A260/A230 absorption ratio, the highest absorption ratio resulting in the highest purity, was found by 50  $\mu\text{L}$  of ambient air between each washing solvent during the flow washing concept. The averaged **DNA-2b** recoveries after flow washing/elution (FW) were calculated and plotted in the bar chart Fig. 6 A-b) to determine

qualitative DNA recovery. The same pattern in the bar plot represents samples from the same stock solution, making the flow samples comparable to the corresponding batch references. The bar plot confirmed the previously observed qualitative effect that the highest yield of **DNA-2b** was recovered using 50  $\mu\text{L}$  of ambient air between each solvent. The DNA recovery in flow was  $429 \pm 25$  pmol, providing comparable recoveries with high precision to the batch reference sample of  $436 \pm 16$  pmol. Thus, in the following, the volume of ambient air was set to 50  $\mu\text{L}$  for flow washing.

The second set of experiments focused on the volumetric flow rate of the washing solvents, which varied in the range of  $1.0 \text{ mL min}^{-1}$  to  $3.0 \text{ mL min}^{-1}$ . Figure 6 B shows the quantitative and qualitative DNA recovery parameters. For all purified samples analyzed by UV-Vis spectroscopy confirmed the successful affinity-based purification of **analyte-DNA-2b** independent of the volumetric flow rate of the washing solvents. This underlines the robustness of the Watson-Crick interaction based-purification process, as only little loss of the analyte-DNA was observed (ESI Table S 4). The best A260/A230 ratio was obtained for the samples purified at solvent volumetric flow rates of  $1.5 \text{ mL min}^{-1}$  (ratio = 1.29) and  $2.0 \text{ mL min}^{-1}$  (ratio = 1.27). The samples purified with  $1.0 \text{ mL min}^{-1}$  (ratio = 1.10) and  $3.0 \text{ mL min}^{-1}$  (ratio = 1.16) showed the lowest A260/A230 ratio in this set of experiments. The bar plot showing qualitative DNA recoveries confirms this trend (Fig. 6 B-b). Here, the highest DNA recoveries were found at a flow rate of  $1.5 \text{ mL min}^{-1}$  with  $429 \pm 25$  pmol and  $2.0 \text{ mL min}^{-1}$  with  $419 \pm 19$  pmol. Comparison with the corresponding batch reference from the same stock solution (same patterns in the bars) underlines comparable **DNA-2b** recoveries with high precision, as confirmed in the parity plot (Fig. 6 B-c). Based on these

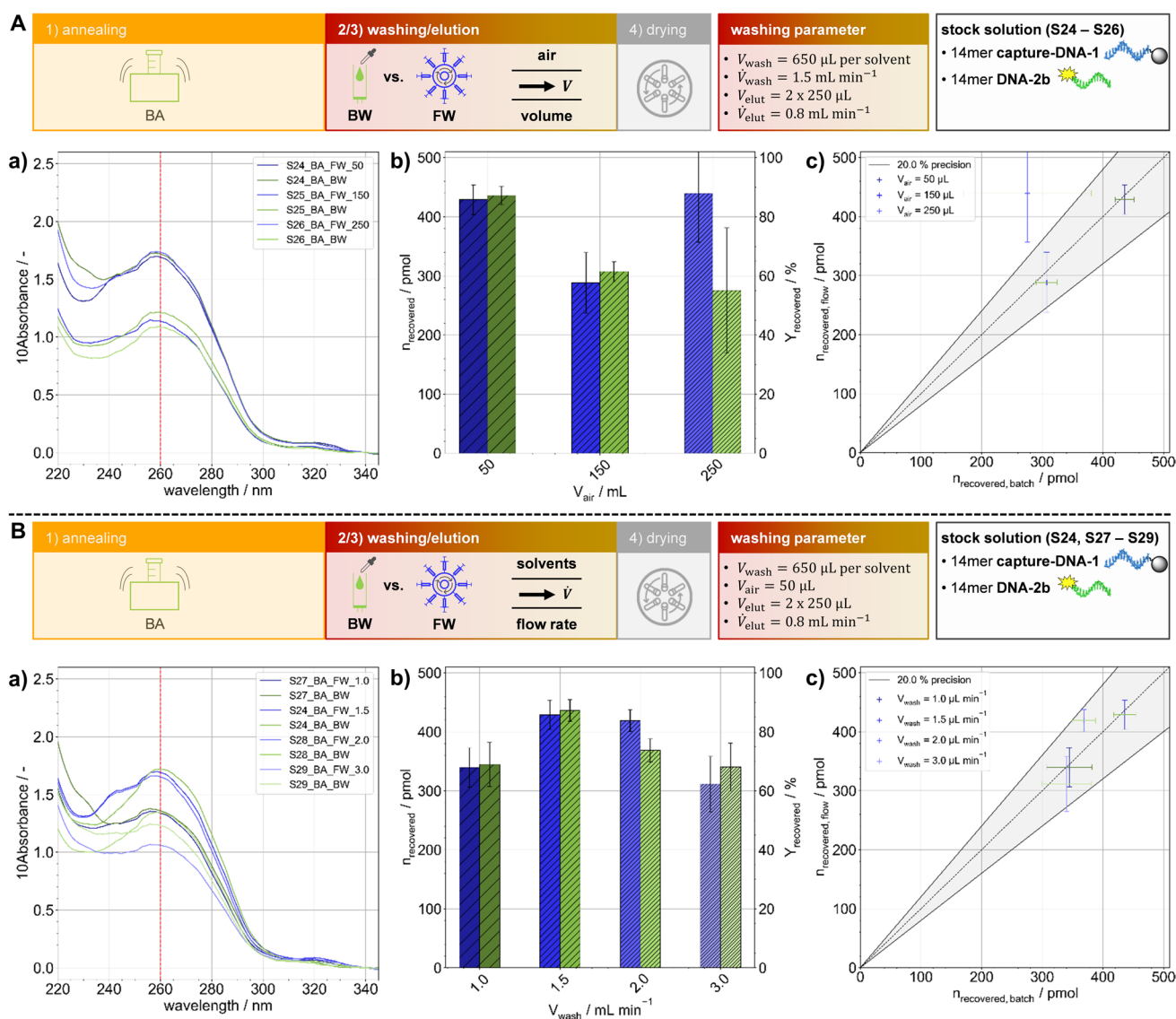


**Fig. 6** Characterization and comparison of the relevant parameters on the flow washing/elution concept. The stock solutions (S) samples were incubated in batches to anneal the **analyte-DNA-2b** (500 pmol) to the **capture-DNA-1**. The annealed analyte-matrix-complex was continuously washed in flow (FW), and in parallel discontinuously in batch (BW) to compare the both washing/elution modes directly: **a)** UV-Vis absorbance spectrum with quantitative DNA recovery; **b)**

bar plot with qualitative DNA recovery ( $n_{recovered}$  in pmol,  $Y_{recovered}$  in %) calculated by the absorbance spectrum at A260; **c)** parity plot for comparing the qualitative DNA recovery after flow and batch annealing. **A)** Investigation of three increasing volumes of ambient air to separate the pure organic washing solvents. **B)** Investigation of five increasing volumetric flow rates of the washing solvents on the flow washing/elution

results, a volumetric flow rate for the combined mode of flow annealing and flow washing/elution was set to  $1.5 \text{ mL min}^{-1}$ .

Excellent DNA recoveries of over 80% were achieved with the newly developed flow concept for washing/elution of analyte-DNA using  $50 \mu\text{L}$  of ambient air between each solvent and a volumetric flow rate of the solvents of  $1.5 \text{ mL min}^{-1}$ . It was confirmed that the washing/elution solvents did not introduce contamination into the microfluidic purification process and thus had no effect on the purity of the analyte-DNA. The head-to-head comparison of the samples purified by the

microfluidic process and the batch references averaged inside the precision range. Therefore, the flow washing/elution concept was very well applicable for performing affinity-based purification steps in DEL-synthesis.

### Automatable Flow Affinity-Based Purification

Finally, the previously individually verified flow annealing and washing/elution concepts were combined and connected using a three-port valve (V3). In this way, performing an

automatable flow affinity-based purification of DNA-tagged substrates was possible. For the automation strategy, several tailored open-source sensors and actuators were built and integrated into the flow process to ensure reproducible experimental procedure, monitoring, and control of the microfluidic affinity-based purification process, as shown in Fig. 7 A.

Physical computing and do-it-yourself lab-ware [26–28] have used open-source hardware and software for low-cost microfluidic automation. In this work, a Pt100 temperature sensor (TI) connected to an amplifier board and Arduino microcontroller-board (MCB) monitors the water bath

temperature during annealing. The photo resistance flow sensor (FI) developed by Höving *et al* [29], monitors the back and forth pumping during incubation, as explained in Section "Flow annealing concept". A peristaltic pump (P1) was connected via an RS232-to-USB converter, and a self-written Python library controlled the pump (P1) and set the volumetric flow rate (ESI Section 3.3.1). The multi-port valve (V1) for washing/elution was automated using stepper motor drivers connected to an Arduino MCB. Two three-port valves (V2, V3) were tailored to the process by open-source automation and driven by servo

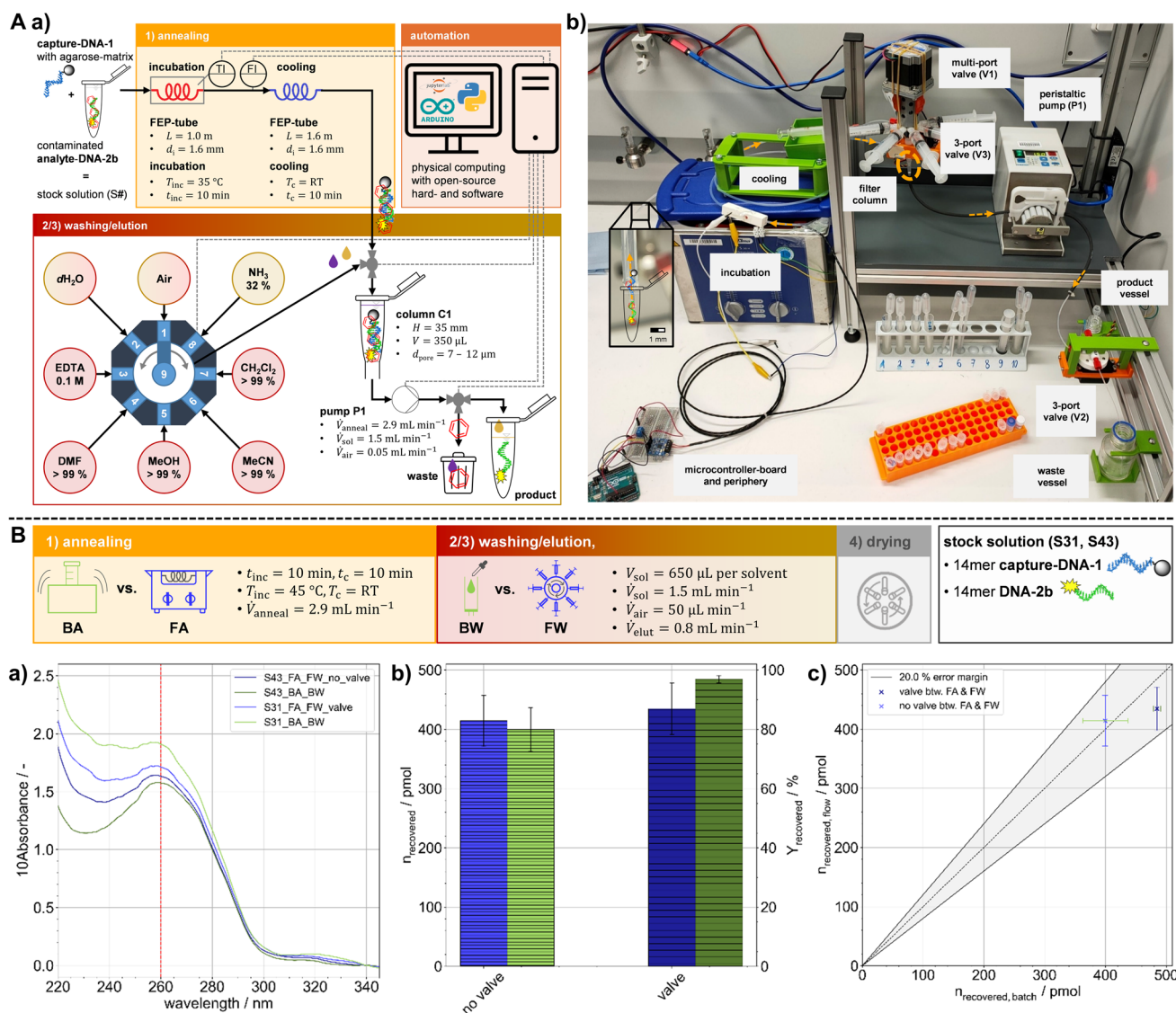


**Fig. 7** Overview and comparison of the automatable continuous affinity-based purification process of DNA-tagged substrates. **A)** Schematic structure of the automated microfluidic annealing and washing/elution concept. **a)** Automation strategy with tailored sensors and actuators. **b)** Experimental setup, the arrows indicate the flow direction. **B)** Characterization of the complete automated continuous affinity-based purification process of 500 pmol **analyte-DNA-2b**

with tailored sensors and actuators. Comparison of flow purified samples (FA\_FW) in blue colors with corresponding batch purified samples (BA\_BW) in blue colors. **a)** UV-Vis absorbance spectrum with quantitative DNA recovery; **b)** bar plot with qualitative DNA recovery ( $n_{\text{recovered}}$  in pmol,  $Y_{\text{recovered}}$  in %) calculated by the absorbance spectrum at A260; **c)** parity plot for comparing the qualitative DNA recovery after flow and batch annealing

motors connected to another Arduino. The first three-port valve (V2) was installed between flow annealing and flow washing/elution to load the filter column (C1) with the analyte-matrix-complex. The second three-port valve (V3) switched from washing to elution for collecting the purified **analyte-DNA-2b**. A detailed overview of the installed sensors and actuators, including the automation strategy in Python can be found in the ESI Section 3.3.1.

In Fig. 7 B, the final set of experiments focused on combining the previously developed flow annealing and washing/elution concept using an automation strategy. The experiments were repeated with and without the automated three-port valve (V3) between the flow annealing and washing/elution concept. The qualitative and quantitative DNA recovery parameters aimed for comparable DNA recoveries of purified **DNA-2b** in batch and flow. Two triplicates ( $2 \times 3$  samples) were prepared from a new stock solution and purified by batch (BA\_BW) and flow (FA\_FW) concepts. A first look at the averaged absorption spectra indicates as a quantitative parameter (Fig. 7 B-a) that both the flow and reference batch samples were purified successfully, confirming the previous findings. The calculated yield of DNA recovery as a qualitative parameter (Fig. 7 B-b,c) shows the effective automation of the flow annealing and the flow washing/elution in a high precision range. First, analyte-DNA was purified by manual reconnection of the automated flow annealing and washing/elution concepts. Concerning the results of the validation experiments (Fig. 4, Fig. 6, Fig. 7), comparable DNA recoveries were observed with high precision in this set of experiments, as seen in the parity plot. To avoid the manual transfer of the sample to the filter column (C1) for flow washing/elution after flow annealing, a tailored and automated three-port valve (V3) was installed to recover DNA with minimal loss in flow ( $435 \pm 35$  pmol), satisfactorily combining automated flow annealing and washing/elution. These results pave the way toward integrating the affinity-based purification process into an automated synthesis platform for DNA-encoded library synthesis.

## Conclusion and Outlook

The purification of DNA-tagged substrates is an essential step in DNA-encoded chemistry. This work was motivated to transfer the established affinity-based batch purification process based on DSPE for DEL technology by Götte *et al* [5, 12], into an automatable continuous flow process for purifying DNA-conjugates in the microliter range. In this contribution, automated microfluidic annealing and washing/elution concepts were developed and evaluated for DNA-encoded chemistry efficiently using open-source lab automation and tailored 3D-printed equipment for the first time. This work aimed at comparing batch and flow

purification processes regarding DNA recovery and purity by determining qualitative (absorbance spectra) and quantitative (recovered amount of substance) parameters. First, the annealing step of the DSPE was transferred from batch to flow by binding an ssDNA to an agarose-matrix, called capture-DNA, which was then bound to an analyte-DNA via Watson–Crick interactions. The results confirm that comparable analyte-DNA recoveries were achieved in both batch and flow using the flow annealing concept as the first step of the DSPE. The application of the new flow annealing concept was verified with longer analyte-DNA strands. It revealed the same trend of decreasing DNA recoveries as the batch reference for longer analyte-DNA strands. Next, the relevant parameters of the flow washing process were optimized for thoroughly washing the bound analyte-DNA with various aqueous and organic solvents and removing impurities and contaminations of different polarities. The purified analyte-DNA was then isolated from the fully complementary DNA-strand and the solid-phase by the elution solvent  $\text{NH}_3(\text{aq})$ . Head-to-head comparison of purified analyte-DNA in the batch and flow process yielded comparable and high and precise DNA recoveries of over 80%.

The feasibility of affinity-based purification of DNA-tagged substrates was successfully demonstrated using microfluidic annealing and washing/elution concepts with DNA-tagged substrates for the first time. Further studies will investigate how much the organic washing/elution solvents could be reduced without affecting DNA recovery to reduce drying time and save resources. The microfluidic affinity-based purification process for DEL technology may be used for purifying DELs encoded with a double-stranded DNA by adding a single-stranded region to the DNA-barcode [5]. In addition, it remains to be shown that the flow affinity-based purification is universally applicable to the field of DEL chemistry, particularly robust enough for DNA reaction products such as the amide coupling reaction conducted in our groups [4, 5, 30]. Götte *et al* [5], have already demonstrated the feasibility of batch affinity-based purification of amide coupling products with DNA-tagged substrates. The current focus is on the flow affinity-based purification of amide coupling products, combining automated microfluidic purification with an automated two-phase reaction system for DNA-tagged substrates and integration it into an automated flow chemistry platform for DEL technologies [4, 31].

**Abbreviations**  $\text{CH}_2\text{Cl}_2$ : Dichloromethane; CPG: Controlled pore glass; DEL: DNA-encoded library; DMF: Dimethylformamide; DNA: Deoxyribonucleic acid; DSPE: Dispersive solid-phase extraction; EDTA: Ethylenediaminetetraacetate; FEP: Fluoroethylene propylene; FI: Photo resistance flow sensor; HPLC: High performance liquid chromatography; HTS: High-throughput screening; MCB: Microcontroller-board; MeCN: Acetonitrile; MeOH: Methanol;  $\text{NH}_3(\text{aq})$ : Aqueous ammonia; RSD: Relative standard deviation; RT: Room temperature; SPE: Solid-phase extraction; ss: Single-stranded; TI: Temperature sensor

**Supplementary Information** The online version contains supplementary material available at <https://doi.org/10.1007/s41981-023-00282-0>.

**Acknowledgements** The authors thank the German Research Foundation (DFG) for financial support under Grants KO2349/18 and BR5049/7-1 and Carsten Schrömgies for his technical support.

**Author contributions** The manuscript was written through contributions of all authors. All authors have given approval to the final version of the manuscript.

**Funding sources** Open Access funding enabled and organized by Projekt DEAL. The authors thank the German Research Foundation (DFG) for financial support under Grants KO2349/18 and BR5049/7-1.

**Open Access** This article is licensed under a Creative Commons Attribution 4.0 International License, which permits use, sharing, adaptation, distribution and reproduction in any medium or format, as long as you give appropriate credit to the original author(s) and the source, provide a link to the Creative Commons licence, and indicate if changes were made. The images or other third party material in this article are included in the article's Creative Commons licence, unless indicated otherwise in a credit line to the material. If material is not included in the article's Creative Commons licence and your intended use is not permitted by statutory regulation or exceeds the permitted use, you will need to obtain permission directly from the copyright holder. To view a copy of this licence, visit <http://creativecommons.org/licenses/by/4.0/>.

## References

- Satz AL, Brunschweiler A, Flanagan ME, Gloger A, Hansen NJV, Kuai L, Kunig VBK, Lu X, Madsen D, Marcaurelle LA, Mulrooney C, Odonovan G, Sakata S, Scheuermann J (2022) *Nat Rev Methods Prim* 2:1–17
- Potowski M, Losch F, Wünnemann E, Dahmen JK, Chines S, Brunschweiler A (2019) *Chem Sci* 10:10481–10492
- Potowski M, Kunig VBK, Losch F, Brunschweiler A (2019) *Medchemcomm* 10:1082–1093
- Dinter R, Willems S, Hachem M, Streltsova Y, Brunschweiler A, Kockmann N (2023) *React. Chem Eng* 8:1334–1340
- Götte K, Dinter R, Justen L, Kockmann N, Brunschweiler A (2022) *ACS Omega* 7:28369–28377
- Potowski M, Kunig VBK, Eberlein L, Vakalopoulos A, Kast SM, Brunschweiler A (2021) *Angew Chemie Int Ed* 60:19744–19749
- Gagnon P (2020) Purification of Nucleic Acids: A handbook for purification of plasmid DNA and mRNA for gene therapy and vaccines - Sartorius BIA Separations, BIA Separations. <https://www.biaseparations.com/en/products/monolithic-columns/books/226/purification-of-nucleic-acids-a-handbook-for-purification-of-plasmid-dna-and-mrna-for-gene-therapy-and-vaccines>
- Flood DT, Asai S, Zhang X, Wang J, Yoon L, Adams ZC, Dillingham BC, Sanchez BB, Vantourout JC, Flanagan ME, Piotrowski DW, Richardson P, Green SA, Shenvi RA, Chen JS, Baran PS, Dawson PE (2019) *J Am Chem Soc* 141:9998–10006
- Buller F, Mannocci L, Scheuermann J, Neri D (2010) *Bioconjug Chem* 21:1571–1580
- Franzini RM, Ekblad T, Zhong N, Wichert M, Decurtins W, Nauer A, Zimmermann M, Samain F, Scheuermann J, Brown PJ, Hall J, Gräslund S, Schüler H, Neri D (2015) *Angew Chemie Int Ed* 54:3927–3931
- Yakovchuk P, Protozanova E, Frank-Kamenetskii MD (2006) *Nucleic Acids Res* 34:564–574
- Götte K (2022) Amphiphile Block-Copolymere und eine Affinitäts-Aufreinigung für die DNA-kodierte Chemie, PhD Thesis, TU Dortmund University. <https://eldorado.tu-dortmund.de/handle/2003/41206>
- Fregel R, González A, Cabrera VM (2010) *Electrophoresis* 31:1350–1352
- Li Y, Chen S, Liu N, Ma L, Wang T, Veedu RN, Li T, Zhang F, Zhou H, Cheng X, Jing X (2020) *Biotechniques* 68:191–199
- Potowski M, Kunig VBK, Eberlein L, Škopić MK, Vakalopoulos A, Kast SM, Brunschweiler A (2022) *Front Chem* 10:641
- Korenč M, Mencin N, Puc J, Skok J, Nemeč KŠ, Celjar AM, Gagnon P, Štrancar A, Sekirnik R (2021) *Cell Gene Ther Insights* 7:1207–1216
- Gagnon P, Goričar B, Peršič Š, Černigoj U, Štrancar A (2020) *Cell Gene Ther Insights* 6:1035–1046
- Rocha FRP, Batista AD, Melchert WR, Zagatto EAG (2018) *An Acad Bras Cienc* 90:803–824
- Cabrera LDC, Caldas SS, Prestes OD, Primel EG, Zanella R (2016) *J Sep Sci* 39:1945–1954
- Šalić A, Zelić B (2018) *Food Technol Biotechnol* 56:464–479
- González A, Avivar J, Maya F, Palominocabello C, Turnes Palomino G, Cerdà V (2017) *Anal Bioanal Chem* 409:225–234
- Heptinstall J, Rapley R (2000) *Nucleic Acid Protoc. Handbook*, pp 57–60. <https://link.springer.com/book/10.1385/1592590381>
- Kibbe WA (2007) *Nucleic Acids Res* 35:43–46
- Safety Data Sheet: Dichloromethane ROTISOLV® HPLC. <https://www.carlroth.com/medias/SDB-7334-IE-EN.pdf>. Accessed 28 April 2023
- Safety Data Sheet: Ammonia solution 32% EMPLURA®. <https://www.sigmaldrich.com/DE/de/product/mm/105426>. Accessed 28 April 2023
- Nesterenko PN (2020) *Pure Appl Chem* 92:1341–1355
- Baden T, Chagas AM, Gage G, Marzullo T, Prieto-Godino LL, Euler T (2015) *PLOS Biol* 13:e1002086
- Coakley M, Hurt DE (2016) *J Lab Autom* 21:489–495
- Höving S, Bobers J, Kockmann N (2022) *J Flow Chem* 12:185–196
- Li Y, Gabriele E, Samain F, Favalli N, Sladojevich F, Scheuermann J, Neri D, Comb ACS (2016) *Sci* 18:438–443
- Bobers J, Škopić MK, Dinter R, Sakthithasan P, Neukirch L, Gramse C, Weberskirch R, Brunschweiler A, Kockmann N, Comb ACS (2020) *Sci* 22:101–108

**Publisher's note** Springer Nature remains neutral with regard to jurisdictional claims in published maps and institutional affiliations.